Research Article

Optimization of PEGylation Conditions for BSA Nanoparticles Using Response Surface Methodology

Hasan Kouchakzadeh,[1] Seyed Abbas Shojaosadati,[1,2] Amir Maghsoudi,[1] and Ebrahim Vasheghani Farahani[1]

Abstract. Chemical coupling of polyethylene glycol (PEG) to proteins or particles (PEGylation), prolongs their circulation half-life by greater than 50-fold, reduces their immunogenicity, and also promotes their accumulation in tumors due to enhanced permeability and retention effect. Herein, phase separation method was used to prepare bovine serum albumin (BSA) nanoparticles. PEGylation of BSA nanoparticles was performed by SPA activated mPEG through their free amino groups. Effect of process variables on PEGylation efficiency of BSA nanoparticles was investigated and optimized through response surface methodology with the amount of free amino groups as response. Optimum conditions was found to be 32.5 g/l of PEG concentration, PEG-nanoparticle incubation time of 10 min, incubation temperature of 27°C, and pH of 7 for 5 mg of BSA nanoparticles in 1 mL phosphate buffer. Analysis of data showed that PEG concentration had the most noticeable effect on the amount of PEGylated amino groups, but pH had the least. Mean diameter and zeta potential of PEGylated nanoparticles under these conditions were 217 nm and −14 mV, respectively. In conclusion, PEGylated nanoparticles demonstrated reduction of the negative surface charge compared to the non modified particles with the zeta potential of −31.7 mV. Drug release from PEGylated nanoparticles was almost slower than non-PEGylated ones, probably due to existence of a PEG layer around PEGylated particles which makes an extra resistance in opposition to drug diffusion.

KEY WORDS: 5-fluorouracil; BSA nanoparticle; PEGylation optimization; response surface method (RSM).

INTRODUCTION

The field of drug delivery is fast expanding, and its potentials have already been proven by the many products in the market. Colloidal drug delivery systems (CDDS) such as nano-structures have been developed in order to improve the efficiency and the specificity of drug action. Their small size permits them to be injected intravenously to reach target tissues. Among them, nanoparticulate systems based on proteins have gained much interest because of their inherent properties of biodegradability, lack of toxicity, and non-antigenicity (1,2). Protein nanoparticles may be used as a matrix in which a wide variety of drugs can be physically entrapped (3–5). In contrast to other nanoparticulate systems, they offer the benefit of carrying functional groups such as amino and carboxylic groups that can be used for surface modification (6–8). However, it is known that they can be rapidly removed from the blood circulation by the action of the immune system. CDDS are removed via the complement system and via the cells of the mononuclear phagocyte system, after their recognition by opsonins and/or receptors present at the cell surface. This recognition is dependent on the physicochemical characteristics of the CDDS (9–12).

There are quite a few important reasons for making long-circulating drug carriers. One of them is to maintain a required level of pharmaceutical agent in the blood for extended time intervals. Then, long-circulating drug-loaded nanoparticles can slowly accumulate in pathological sites with affected and leaky vasculature and facilitate drug delivery in those areas. This phenomenon known as enhanced permeability and retention effect has also been termed as passive targeting or accumulation via an impaired filtration mechanism (13–15). In addition, the prolonged circulation can help to achieve a better targeting for targeted drug carriers by providing more time for their interaction with the target (16).

Chemical modification of pharmaceutical nanocarriers with certain synthetic polymers, such as polyethylene glycol (PEG), is the most frequent way to impart the *in vivo* longevity to drug carriers, as was first suggested for liposomes (17–21). This polymer is nontoxic, non-immunogenic, non-antigenic, highly soluble in water, and FDA approved (22). Hydrophilic polymers have been shown to protect individual molecules and solid particulates from interaction with different solutes. The term "steric stabilization" has been introduced to describe the phenomenon of polymer-mediated protection (23). On the biological level, coating nanoparticles with PEG (PEGylation) sterically hinders interaction of blood components with their surface and reduces the binding of

---

[1] Biotechnology Group, Chemical Engineering Department, Faculty of Engineering, Tarbiat Modares University, P.O. Box 14115-143Tehran, Iran.

[2] To whom correspondence should be addressed. (e-mail: shoja_sa@modares.ac.ir)

plasma protein with PEGylated nanoparticles (24–29). This prevents drug carrier's interaction with opsonins and slows down their fast capture by Reticuloendothelial System (30).

In the present study, bovine serum albumin (BSA) was used for the preparation of nanoparticles because of its well-defined primary structure combined with the advantage of enabling surface modification. Nanoparticles prepared from BSA are versatile carrier systems for drug delivery and can be prepared by an established desolvation process (31,32). BSA offers several target sites for covalent modification such as the free amino groups. Since there is no comprehensive study in the literature concerning the influence of process variables on the protein nanoparticles PEGylation, the effect of process variables on the PEGylation efficiency was investigated and optimum condition for preparing PEGylated nanoparticles was determined using response surface methodology considering the amount of free amino groups as response. Then, 5-fluorouracil (5-FU) was used as a model drug for the investigation of PEGylation effect on drug release profile assessed by a continuous flow method.

MATERIALS AND METHODS

Materials

BSA (fraction V, minimum 98%), glutaraldehyde 8% solution, 2,4,6-trinitrobenzene sulfonic acid (TNBS) 5% aqueous solution, and 5-fluorouracil were purchased from Sigma (Steinheim, Germany). mPEG-Succinimidyl Propionate (mPEG-SPA) with the molecular weight of 5 KDa was obtained from Sunbio (Orinda, USA) and Polysulfone filtration membrane (100 KDa) from Sartorius (Goettingen, Germany). All other reagents were purchased from Merck (Darmstadt, Germany); they were of analytical grade and used as received.

Methods

Preparation of BSA Nanoparticles

BSA nanoparticles were prepared by a desolvation method as described elsewhere (31,32). Briefly, 0.2 g BSA in 2.0 mL aqueous solution, titrated to desired pH, was converted to nanoparticles by continuous addition of desolvating agent, ethanol, at the rate of 1.0 mL/min and under stirring (550 rpm) at room temperature. Subsequently, 8% glutaraldehyde aqueous solution was added to induce particle cross-linking. The cross-linking process was performed under stirring of the suspension over night. 5-FU-loaded BSA nanoparticles were produced by an optimized desolvation process reported in our previous study (32).

Separation of Nanoparticles

Possible microparticles were precipitated by centrifugation (15,000×g, 2 min) and then discarded. Nanoparticles were separated by 2 cycles of centrifugation (25,000×g, 20 min) and redispersion of the pellet to the original volume in 10 mM NaCl pH 9. Each redispersion step was carried out using ultrasonication (dr.hielscher, UP 400S, Germany) for 5 min. Then, BSA nanoparticles solution was freeze-dried to yield nanoparticle powder.

Free Amino Group Quantification of Nanoparticles

Determination of amino groups was performed using the reaction of TNBS with free amino groups (33–35). In principle, 250 μl aqueous 0.01% TNBS solution was added to the 500 μl of 0.5 mg/mL nanoparticle in 0.1 M sodium bicarbonate buffer (pH 8.5). The reaction mixture was shaken at 500 rpm for 2 h at 37°C. In order to separate the nanoparticles, the sample was centrifuged (35,000×g, 30 min). The supernatant was assayed spectrophotometrically at 345 nm for unreacted TNBS. Free amino group content of particles was calculated relative to a TNBS reference that was treated in the same manner as described above, using water instead of the particle solution.

PEGylation Optimization of Nanoparticles

PEG concentration, incubation time, reaction temperature, and pH have been considered as the most important factors for further investigation by response surface method using central composite design (CCD; four factors and five levels; Table I), considering the amount of free amino groups as response. Each trial was performed twice. Concentration of nanoparticle solution was constant in all experiments at 5 g/L (36,37).

The values of levels of all factors were chosen according to a previous research (36) and several preliminary experiments. Measuring free amino groups by TNBS revealed that the molar ratio of free amino group per bare BSA nanoparticle is 7.86. So based on the concentration of nanoparticles (5 g/L) and assuming molar ratio range of 1–10 for PEG per amino group, the lowest and highest levels of PEG concentration was calculated to be 2.5 and 32.5 g/L, respectively.

mPEG-SPA with the molecular weight of 5,000 Da was used for conjugation to nanoparticles. Due to high sensitivity of activated PEG to moisture, dried acetone was used as PEG solvent (37). Ethanolamine solution (98%), 10 μL, was added to samples to terminate the reaction. PEG conjugated BSA nanoparticles were purified by centrifugation at 35,000×g for 17 min followed by redispersion in 0.1 sodium bicarbonate buffer (pH 8.5). Dispersed solution was diluted to a final nanoparticle concentration of 0.5 mg/mL with 0.1 M sodium bicarbonate (pH 8.5). Free amino group content of modified BSA nanoparticles was measured by TNBS method as described before. By comparison of the resulted amount of free amino groups after PEGylation with the original amount, efficiency of the PEGlation process was calculated as the percentage of PEGylated amino groups.

Table I. Selected Levels and Factors for Central Composite Design of BSA Nanoparticles PEGylation

	Variables	Coded Value				
		−α (−2)	−1	0	+1	+α (+2)
X_1	C_{PEG} (g/l)	2.5	10	17.5	25	32.5
X_2	t (min)	10	40	70	100	130
X_3	T (°C)	3	9	15	21	27
X_4	Ph	7	7.5	8	8.5	9

Determination of Particle Size and Zeta Potential

Average size and zeta potential of bare nanoparticles and PEGylated nanoparticles in optimum condition was measured by photon correlation spectroscopy using a Malvern zetasizer 3000HS (Malvern Instrument Ltd, UK). The samples were measured at a temperature of 25°C and a scattering angle of 90°.

In Vitro Drug Release Profile

In two separate experiments, PEGylated and bare 5-FU-loaded nanoparticles were injected to an ultrafiltration system (Fig. 1) consisted of two membranes (5 cm diameter and 100 KDa cutoff) with 1 mm distance and was immersed in 100 mL phosphate-buffered saline pH 7.4. This setup was placed in an incubator (N-Biotech, NB-205, Belgium) at 37°C and agitated at 100 rpm by a magnetic stirrer. The release medium was withdrawn at the rate of 0.1 mL/min by an HPLC pump and assessed continuously for 5-FU concentration with a UV-Vis detector (M730D, Younglin Instrument, Korea) for 1,400 min. The detector was set at 265 nm with a sensitivity of 1.00 absorbance unit full scale and a sampling rate of 4 Hz. For maintaining sink conditions, fresh buffer was added at the same rate with a syringe pump (World Precision Instruments, SP200i, USA). Drug release experiments from both bare and PEGylated nanoparticles were conducted in duplicate, and the averages of release profiles were considered for the study of PEGylation effect on the drug release.

RESULTS AND DISCUSSION

Nanoparticles PEGylation Optimization

According to literature, PEG concentration, incubation time, temperature, and pH were selected as the independent input variables and free amino group content as the dependent output variable. Based on the free amino group content of bare nanoparticles, the lowest and highest levels of PEG concentration were determined. In addition, free amino group content of bare nanoparticles was considered as a reference in finding PEGylation process efficiency.

A central composite design was employed to analyze the interactive effect of these parameters and to arrive at an optimum condition. A 2^4-factorial central composite experimental design, with eight axial points and seven replications at the center points leading to a total number of 31 experiments was employed for the optimization of the parameters (38). The variables were coded according to the following equation:

$$X_i = (x_i - x_i^*)/\Delta x_i \qquad (1)$$

Where X_i is the coded value, x_i is the actual value of the *i*th test variable, x_i^* is the value of x_i at the center point of the investigated area, and Δx_i is the step size. The range of the variables is given in Table I. The experimental design protocols (developed by Minitab 15 Software) (39) and corresponding results are presented in Table II.

The experimental results of the CCD were fitted with a second-order polynomial equation. The values of regression coefficients were calculated and the fitted equation (in terms of coded values) for prediction of PEGylation efficiency was as follows:

$$\begin{aligned}
Y = {} & 7.1036 + 1.009X_1 + 0.664X_2 + 0.7606X_3 + 0.2105X_4 \\
& - 0.5035X_1^2 - 0.2943X_2^2 - 0.171X_3^2 - 0.2959X_4^2 \\
& - 0.3077X_1X_2 + 0.0857X_1X_3 + 0.3214X_1X_4 \\
& - 0.2965X_2X_3 + 0.4344X_2X_4 - 0.3998X_3X_4
\end{aligned}$$

$$(2)$$

Where Y is molar ratio of PEGylated amino groups per bare BSA nanoparticles and X_1, X_2, X_3, and X_4 are coded values for PEG concentration, time, temperature, and pH, respectively.

The coefficients of the regression model (Eq. 2) that appear as one constant, four linear, four quadratic, and six interaction terms are listed in Table III. The significance of each coefficient, determined by p values, is also given. The p values imply that the first order main effects of PEG concentration, time, and temperature and second-order main effects of PEG concentration, time, and pH were significant. Of the interaction terms, time–pH was found to be the most significant term.

It is required to test the significance and adequacy of the model through analyses of variance. Fisher variance ratio, the F value, is a statistically valid measure of how well the factors describe the variation in the data about its mean. The greater
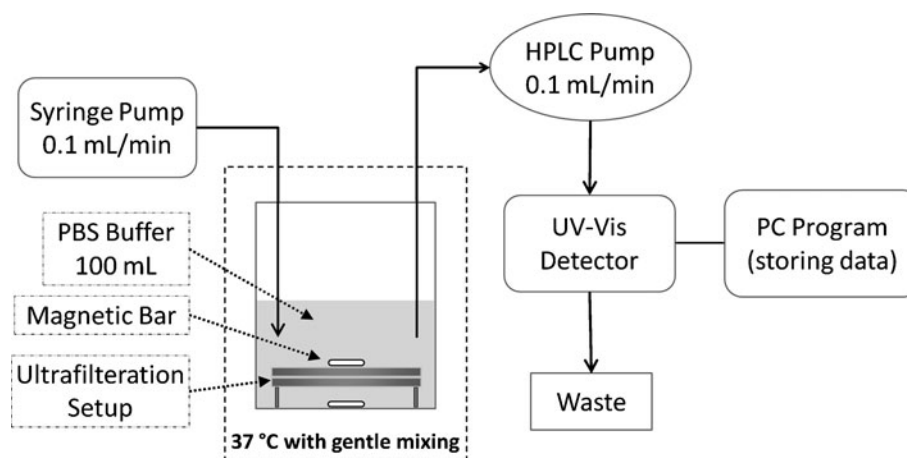

Fig. 1. Schematic representation of the ultrafiltration setup used for assessing drug release profile

Table II. PEGylation Optimization of BSA Nanoparticles Using Central Composite Design

	Coded Factors				Experimental Results	
Trial	X_1	X_2	X_3	X_4	Molar Ratio of PEGylated Amino Groups per bare BSA Nanoparticles	PEGylation Efficiency (%)
1	−1	−1	−1	−1	2.77025	35
2	1	−1	−1	−1	4.2959	54
3	−1	1	−1	−1	4.62282	59
4	1	1	−1	−1	4.96897	63
5	−1	−1	1	−1	6.469	82
6	1	−1	1	−1	7.7767	97
7	−1	1	1	−1	5.6292	71
8	1	1	1	−1	7.43605	94
9	−1	−1	−1	1	2.6741	34
10	1	−1	−1	1	5.7254	73
11	−1	1	−1	1	5.5587	71
12	1	1	−1	1	7.50743	95
13	−1	−1	1	1	3.45615	44
14	1	−1	1	1	7.59077	96
15	−1	1	1	1	6.84077	87
16	1	1	1	1	7.83436	98
17	−2	0	0	0	3.09718	39
18	2	0	0	0	7.64846	95
19	0	−2	0	0	4.63564	59
20	0	2	0	0	7.78308	97
21	0	0	−2	0	5.8664	74
22	0	0	2	0	7.53948	95
23	0	0	0	−2	5.7446	73
24	0	0	0	2	6.6613	85
25	0	0	0	0	7.10359	90
26	0	0	0	0	7.10361	90
27	0	0	0	0	7.1036	90
28	0	0	0	0	7.10359	90
29	0	0	0	0	7.10358	90
30	0	0	0	0	7.10362	90
31	0	0	0	0	7.10359	90

the F value is from unity, the more certain it is that the factors adequately explain the variation in the data around its mean, and the estimated factor effects are real. The analysis of variance of the regression model demonstrates that the model is highly significant, as is evident from the Fisher's F test ($F_{model}=16.36$). The goodness of fit with this quadratic model was confirmed by the determination coefficient (R^2). In this case, the value of the determination coefficient ($R^2=0.935$) indicates that 93.5% of the variability in the response could be explained by the model.

The optimum (coded variables), obtained by Minitab software (version 15) for achieving maximum PEGylation, accrued at $X_1=32.5$, $X_2=10$, $X_3=27$, $X_4=7$. It was predicted that in the optimum condition all of the free amino groups would be PEGylated. To confirm the model accuracy in predicting optimum condition, additional experiments in triplicate were performed at the optimum condition. These experiments yielded an average PEGylation efficiency of 100%. The good agreement between the predicted and experimental results verified the validity of the model and the existence of the optimal point.

Two-dimensional contour plots are the graphical representations of the regression equation and are plotted to understand the interaction of the variables and to locate the optimum level of each variable for maximum response. Each contour represents the different combinations of two test variables at one time while keeping the other two variables at their respective zero level. Two typical counter plots are presented in Fig. 2.

Table III. Analysis of the Central Composite Design Results for PEGylated Nanoparticles

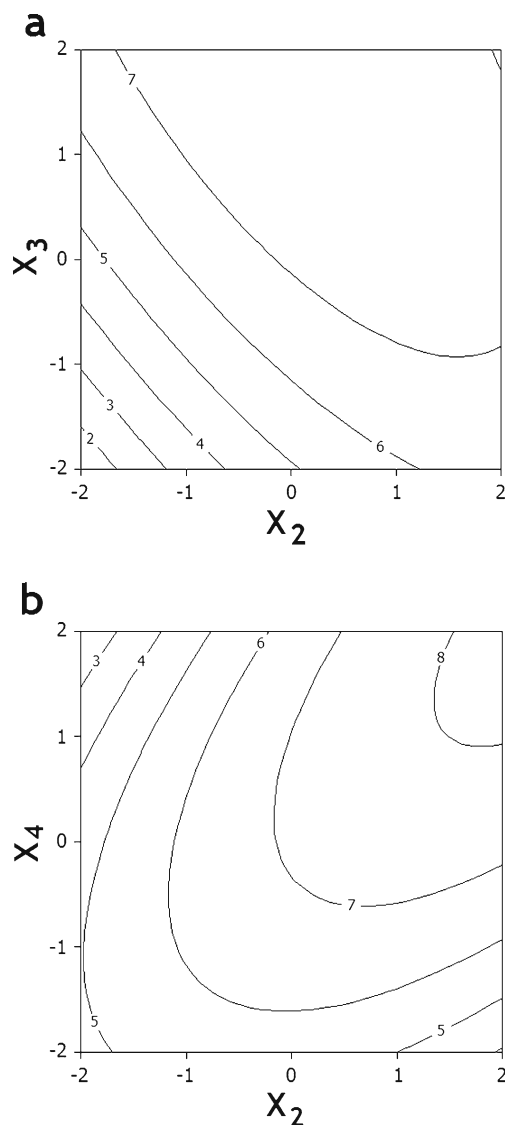| Term	Regression Coefficient	T value	p Value
Intercept	7.1036	33.821	0.000
X_1	1.009	8.896	0.000
X_2	0.664	5.853	0.000
X_3	0.7606	6.706	0.000
X_4	0.2105	1.856	0.082
X_1*X_1	−0.5035	−4.845	0.000
X_2*X_2	−0.2943	−2.832	0.012
X_3*X_3	−0.171	−1.645	0.119
X_4*X_4	−0.2959	−2.848	0.012
X_1*X_2	−0.3077	−2.515	0.042
X_1*X_3	0.0857	0.617	0.546
X_1*X_4	0.3214	2.313	0.034
X_2*X_3	−0.2965	−2.134	0.049
X_2*X_4	0.4344	3.127	0.007
X_3*X_4	−0.3998	−2.878	0.011

Fig. 2. Contour plots of variables in BSA nanoparticles PEGylation, **a** for the interaction between t (X_2) and T (X_3), and **b** for the interaction between t (X_2) and pH (X_4) at zero level of the other two variables

Particle Size and Zeta Potential of PEGylated and Bare Nanoparticles

Mean diameter and zeta potential of bare nanoparticles were 210 nm and −31.7 mV, respectively. In contrast, mean diameter and zeta potential of PEGylated nanoparticles under optimum condition were 217 nm and −14 mV, respectively. As results reveal, PEG-BSA nanoparticles demonstrated reduction of the negative surface charge compared to the non-modified nanoparticles, but mean diameter of bare and PEGylated particles are approximately the same. The zeta potential Reduction after PEGylation is due to the surface coating of nanoparticles by PEG molecules.

In Vitro **Drug Release**

5-FU release from bare and PEGylated nanoparticles was accomplished as described before. The averages of 5-FU release profiles are presented in Fig. 3. In this figure, *y*-axis is the 5-FU concentration in the output flow, which is obtained from the conversion of voltage to concentration unit by a standard curve. According to this figure, comparison of profiles shows that drug release from PEGylated nanoparticles is to some extent slower than that of bare nanoparticles. Probably this phenomenon is due to the presence of a PEG layer around PEGylated nanoparticles that may produce an additional resistance against drug transport from particle surface.

CONCLUSION

Preparation process for PEGylated BSA nanoparticles was studied by response surface method using central composite design. Optimum production condition of PEGylated BSA nanoparticles for 5 g/L of particles was as follows: 32.5 g/L mPEG-SPA 5,000 Da, 10 min incubation time, 27°C incubation temperature and pH 7. This leads to production of PEGylated nanoparticles with mean size of 217 nm and zeta potential of −14 mV, which showed reduction of the negative surface charge compared to the bare particles. Therefore, to some extent, PEG coating masked the negative charge of nanoparticles. Drug release profiles demonstrated that drug release from PEGylated nanoparticles is slower than bare nanoparticles, probably due to the presence of a PEG layer around PEGylated particles.
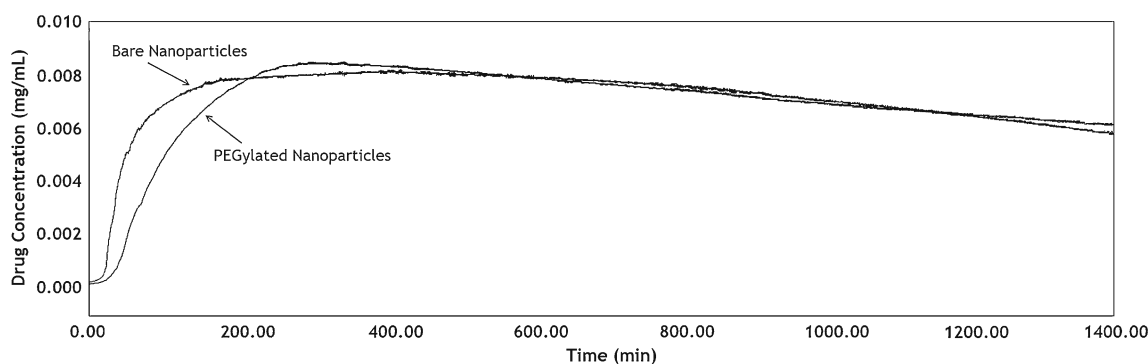

Fig. 3. Drug release profiles from bare and PEGylated nanoparticles

ACKNOWLEDGMENTS

REFERENCES

1. Muller BG, Leuenberger H, Kissel T. Albumin nanospheres as carriers for passive drug targeting: an optimized manufacturing technique. Pharm Res. 1996;13:32–7.
2. Patil GV. Biopolymer albumin for diagnosis and in drug delivery. Drug Dev Res. 2003;58:219–47.
3. Merodio M, Arnedo A, Renedo MJ, Irache JM. Ganciclovir-loaded albumin nanoparticles: characterization and *in vitro* release. Eur J Pharm Sci. 2001;12:251–9.
4. Merodio M, Irache JM, Valamanesh F, Mirshahi M. Ocular disposition and tolerance of ganciclovir-loaded albumin nanoparticles after intravitreal injection in rats. Biomaterials. 2002;23: 1587–94.
5. Lin W, Garnett MC, Davis SS, Schacht E, Ferruti P, Illum L. Preparation and characterization of rose Bengal-loaded surface-modified albumin nanoparticles. J Control Release. 2001;71:117–26.
6. Wartlick H, Michaelis K, Balthasar S, Strebhardt K, Kreuter J, Langer K. Highly specific HER2-mediated cellular uptake of antibody-modified nanoparticles in tumour cells. J Drug Target. 2004;12:461–71.
7. Dreis S, Rothweiler F, Michaelis M, Cinatl J Jr, Kreuter J, Langer K. Preparation, characterization and maintenance of drug efficacy of doxorubicin-loaded human serum albumin (HAS) nanoparticles. Int J Pharm. 2007;341:207–14.
8. Weber C, Reiss S, Langer K. Preparation of surface modified protein nanoparticles by introduction of sulfhydryl groups. Int J Pharm. 2000;211:67–78.
9. Vonarbourg A, Passirani C, Saulnier P, Benoit JP. Parameters influencing the stealthiness of colloidal drug delivery systems. Biomaterials. 2006;27:4356–73.
10. Dumitriu S. Polymeric biomaterials. New York: Marcel Dekker; 2001.
11. Stolnik S, Illum L, Davis S. Long-circulating microparticle drug carriers. Adv Drug Deliv Rev. 1995;16:195–214.
12. Pasut G, Veronse FM. Polymer-drug conjugation, recent achievements and general strategies. Prog Polym Sci. 2007;32:933–61.
13. Maeda H, Wu J, Sawa T, Matsumura Y, Hori K. Tumor vascular permeability and EPR effect in macromolecular therapeutics, a review. J Control Release. 2000;65:271–84.
14. Maeda H. The enhanced permeability and retention (EPR) effect in tumor vasculature: the key role of tumor-selective macromolecular drug targeting. Adv Enzyme Regul. 2001;41:189–207.
15. Gabizon A. Liposome circulation time and targeting: implication for cancer chemotherapy. Adv Drug Deliv Rev. 1995;16:285–94.
16. Torchilin VP. Multifunctional nanocarriersm. Adv Drug Deliv Rev. 2006;58:1532–55.
17. Klibanov AL, Maruyama K, Torichilin VP, Huang L. Amphipatic polyethyleneglycols effectively prolong the circulation time of liposomes. FEBS Lett. 1990;268:235–8.
18. Maruyama K, Yuda T, Okamoto A, Ishikura C, Kojima S, Iwatsuru M. Effect of molecular weight in amphipathic polyethyleneglyco on prolonging the circulation time of large unilamellar liposomes. Chem Pharm Bull. 1991;39:1620–2.
19. Senior J, Delgado C, Fisher D, Tilcock C, Gregoriadis G. Influence of surface hydrophilicity of liposomes on their interaction with plasma protein and clearance from the circulation: studies with poly (ethylene glycol)-coated vesicles. Biochim Biophys. 1991;1066:77–82.
20. Allen TM, Hanse C, Martin F, Redemann C, Young YA. Liposomes containing synthetic lipid derivatives of poly (ethylene glycol) show prolonged circulation half-lives *in vivo*. Biochem Biophys. 1991;1066:29–36.
21. Papadjopoulos D, Allen TM, Gabizon A, Mayhew E, Matthay K, Huang SK, et al. Sterically stabilized liposomes: improvements in pharmacokinetics and antitumor therapeutic efficiency. Proc Natl Acad Sci U S A. 1991;88:11460–4.
22. Veronese FM, Pasut G. PEGylation, successful approach to drug delivery. Drug Discov Today. 2005;10(21):1451–8.
23. Naper DH. Polymeric stabilization of colloidal dispersion. New York: Academic; 1983.
24. Senior J, Delgado C, Fisher D, Tilcock C, Gregoriadis G. Influence of surface hydrophilicity of liposomes on their interaction with plasma protein and clearance from the circulation: studies with poly (ethylene glycol)-coated vesicles. Biochem Biophys. 1991;1062:77–82.
25. Woodle MC. Surface-modified liposomes: assessment and characterization for increased stability and prolonged blood circulation. Chem Phys Lipids. 1993;64:249–62.
26. Allen TM. The use of glycolipids and hydrophilic polymers in avoiding rapid uptake of liposomes by the mononuclear phagocyte system. Adv Drug Deliv Rev. 1994;13:285–309.
27. Chonn A, Semple SC, Cullis PR. Separation of large unilamellar liposomes from blood components by a spain column procedure: toward identifying plasma proteins which mediate liposome clearance *in vivo*. Biochem Biophys. 1991;1070:215–22.
28. Chonn A, Semple SC, Cullis PR. Association of blood proteins with large unilamellar liposomes *in vivo*: relation to circulation lifetimes. J Biol Chem. 1992;267:18759–65.
29. Lasic DD, Martin FG, Gabizon A, Huang SK, Papahadjopoulos D. Sterically stabilized liposomes: a hypothesis on the molecular origin of the extended circulation times. Biochem Biophys. 1991;1070:187–92.
30. Senior JH. Fate and behavior of liposomes *in vivo*: a review of controlling factors. CRC Crit Rev Ther Drug Carr Syst. 1987;3:123–93.
31. Langer K, Balthasar S, Vogel V, Dinauer N, Von Briesen H, Schubert D. Optimization of the preparation process for human serum albumin (HSA) nanoparticles. Int J Pharm. 2003;257: 169–80.
32. Maghsoudi A, Shojaosadati SA, Vasheghani Farahani E. 5-fluorouracil-loaded BSA nanoparticles: formulation optimization and *in vitro* release study. AAPS PharmSciTech. 2008;9: 1092–6.
33. Habeeb AFSA. Determination of free amino groups of protein by trinitrobenzenesulfonic acid. Anal Biochem. 1966;14: 328–38.
34. Edwards F, Andry MC, Levy MC. Determination of free amino groups content of serum albumin microcapsules using trinitrobenzenesulfonic acid: effect of variations in polycondensation. Int J Pharm. 1993;96:85–90.
35. Edwards F, Andry MC, Levy MC. Determination of free amino groups content of serum albumin microcapsules: effect of variations in reaction time and in terephthaloyl chloride concentration. Int J Pharm. 1994;103:253–7.
36. Harris JM. Advanced PEGylation: polyethylene glycol and derivatives for advanced PEGylation, Nektar Transforming Therapeutic Catalog. 2006.
37. Niemeyer CM. Bioconjugation protocols. New Jersey: Humana; 2004.
38. Montgomery DC. Design and analysis of experiments. New York: Wiley; 2005.
39. Minitab Inc. Minitab software version 15. http//minitab.com. (Accessed 10/03/09).